

## SUPPLEMENTAL MATERIALS

### Supplemental Table S1

### Supplemental Figures S1-S6

**Table S1. Fertilization and blastocyst progression rates for caput and cauda sperm. Related to Figures 1-3.**

	Fertilization (progression of ICSI zygotes to 2-cell stage)	Blastocyst progression (% of 2-cell stage embryos progressing to blastocysts)
Caput	77.8 +/- 1.9% n=1155	60.3 +/- 4.7% n=348
Cauda	75.6 +/- 2.7% n=1181	62.2 +/- 4.9% n=319

## SUPPLEMENTAL FIGURE LEGENDS

### Supplemental Figure S1. Schematic of small RNA changes during sperm development and maturation. Related to Figures 1-7.

A) Top cartoon shows three populations of spermatozoa, from the testis, caput epididymis, and cauda epididymis. Bottom panels show schematics of the major small RNA changes across this developmental trajectory, such as the global transition from piRNAs to tRFs occurring as sperm enter the epididymis. Note that while the majority of tRFs have been shipped to sperm already in the caput epididymis, several highly abundant tRFs (including tRF-Val-CAC, tRF-Val-AAC, and others – (Sharma et al., 2016)) are cauda-specific. Bottom panel shows schematic for microRNA dynamics in the epididymis. While many singleton microRNAs are relatively stable in abundance across these sperm populations, caput sperm exhibit dramatically decreased abundance of a wide variety of microRNAs (Nixon et al., 2015; Sharma et al., 2016), almost all of which are encoded in genomic clusters ranging from clusters of two (miR-15/16, etc.) to 100 kb-scale clusters with close to 20 miRNAs, such as the imprinted X-linked miR-880 cluster. Sperm transiting the epididymis then apparently re-gain a second round of these clustered microRNAs, which occurs via trafficking of epididymosomes from the surrounding epididymal epithelium ((Sharma et al., 2016) and accompanying manuscript).

B) Example of microRNA cluster dynamics in the epididymis. Data from Sharma *et al* 2016 show abundance (in parts per million reads, on a log<sub>10</sub> y axis) in testis, caput

sperm, and cauda sperm, for the microRNAs comprising the miR-880 cluster. Caput to cauda differences in these and other clustered microRNAs have also been documented in (Nixon et al., 2015), and we have reproduced these observations and confirmed that these microRNAs are highly expressed in purified testicular germ cell populations including mature testicular spermatozoa (see Sharma *et al*, accompanying manuscript).

### **Supplemental Figure S2. Zygotic genome activation. Related to Figure 1.**

A) Embryos were generated using ICSI and cultured for precisely 18, 24, or 28 hours following sperm injection into the oocyte. Embryos were then promptly harvested for single-embryo RNA-Seq.

B) In an original pilot experiment, ICSI embryos were generated over the course of roughly six hours on a given day (on several different days), then harvested for RNA-Seq 20 hours after the last sperm injection. These embryos thus span a poorly-staged time window of roughly 20-26 hours post-fertilization, providing samples that “fill in” temporal gaps between the 18, 24, and 28 hour embryos from (A).

C) All 2-cell stage RNA-Seq. Embryos (columns) are sorted according to their correlation with the final ZGA (28 hours/18 hours) profile. The time of embryo collection is indicated as bars above the heatmap – long pink bars correspond to the relatively unstaged embryos.

### **Supplemental Figure S3. Caput vs. Cauda comparisons for 8-cell, morula, and blastocyst stages. Related to Figure 2.**

Scatterplots as in **Figure 2A**, for the indicated developmental stages. Two separate biological replicates, carried out nearly one year apart, are analyzed separately for the blastocyst stage.

### **Supplemental Figure S4. Validation and further analysis of Caput embryo regulatory phenotypes. Related to Figure 2.**

A) Immunofluorescence (IF) validation of Caput effects on HNRNPAB protein expression in the blastocyst. Four panels show HNRNPAB levels, normalized to the Cauda average, for ~50-150 individual nuclei (from at least eight blastocysts for each experiment) for cauda- and caput-derived blastocysts.

B) Sperm origin does not affect cell fate allocation in blastocysts. Box plots are shown as in **Figure 2C** for three sets of lineage marker genes in blastocyst RNA-Seq data, as indicated. With the exception of the significant upregulation observed for the gene encoding the key primitive endoderm transcription factor GATA6, we find no evidence for changes in cell composition between Caput and Cauda blastocysts.

**Supplemental Figure S5. Morula-stage gene expression in testicular ICSI embryos. Related to Figure 4.**

Scatterplot comparing median mRNA abundance in Cauda (x axis) and Testicular ICSI (y axis) embryos, as in **Figures 4C-D**. More detailed analysis of this experiment will be presented elsewhere – most relevant for this study is the absence of the Caput-specific regulatory program in embryos generated using testicular spermatozoa.

**Supplemental Figure S6. Cauda-specific microRNAs rescue Caput defects in blastocyst-stage gene regulation. Related to Figure 6.**

A) Schematic of microinjection experiments. As in **Figure 6A**, but embryos were cultured to the blastocyst stage for single-embryo RNA-Seq.

B) Data for individual blastocyst-stage embryos, plotted as in **Figure 6C**.

C) Scatterplot comparing Caput effects on mRNA abundance (x axis) with effects of cauda-specific microRNAs (y axis), plotted as in **Figure 6D**.

Figure S1

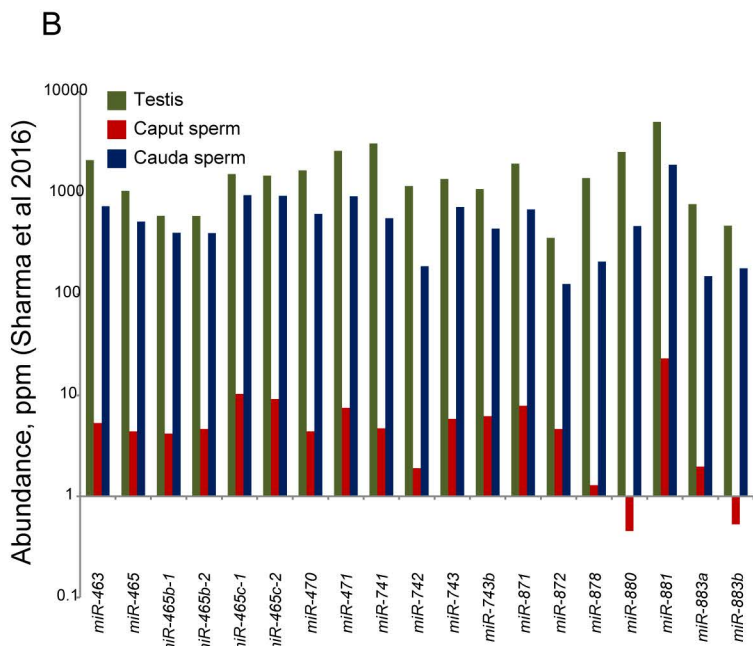
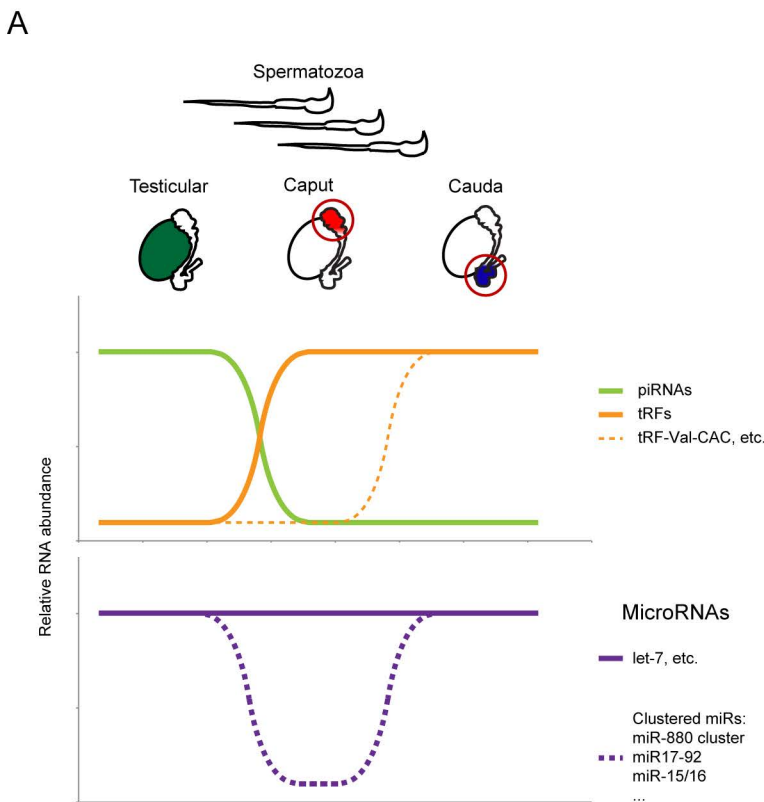


Figure S2

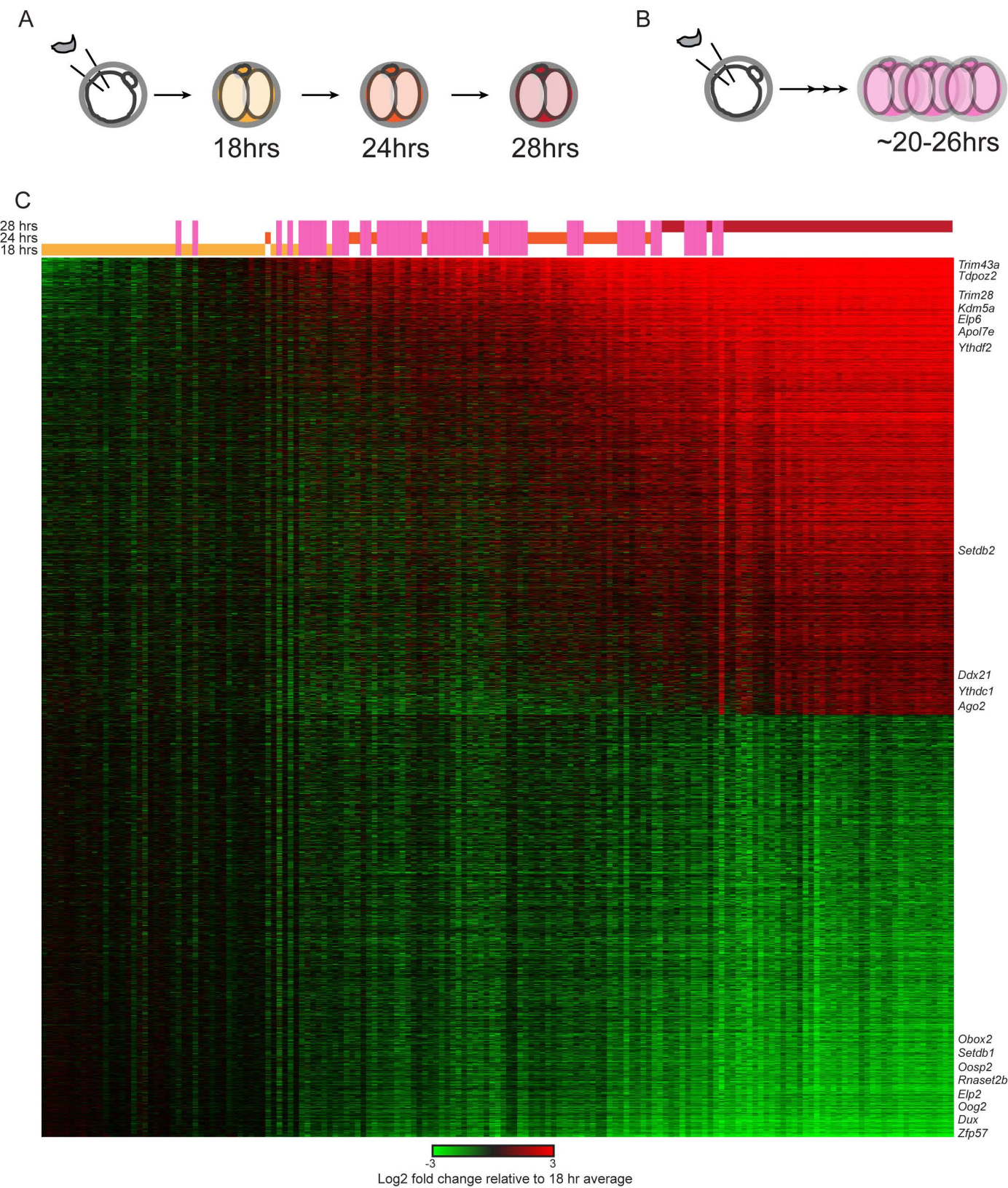


Figure S3

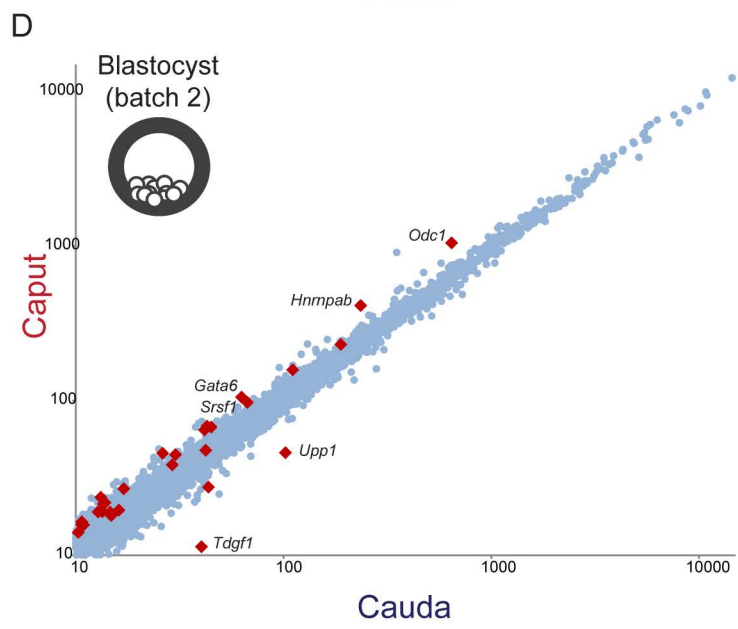
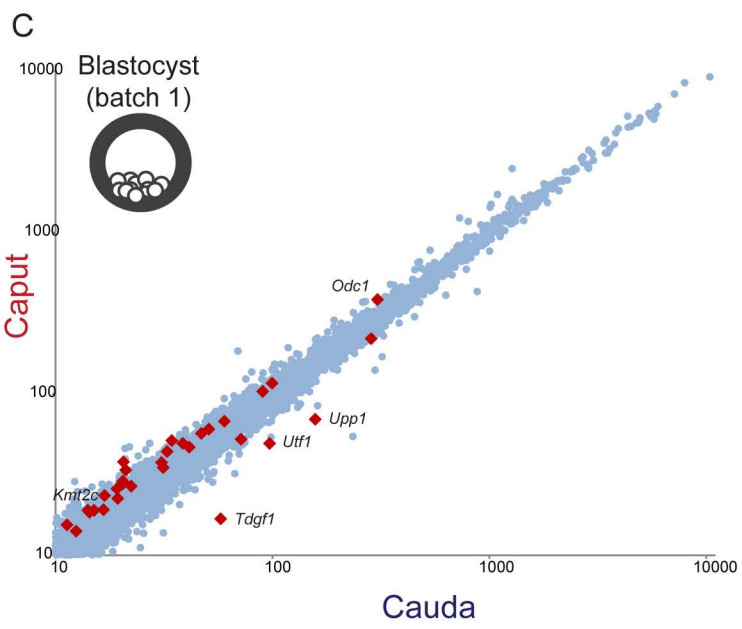
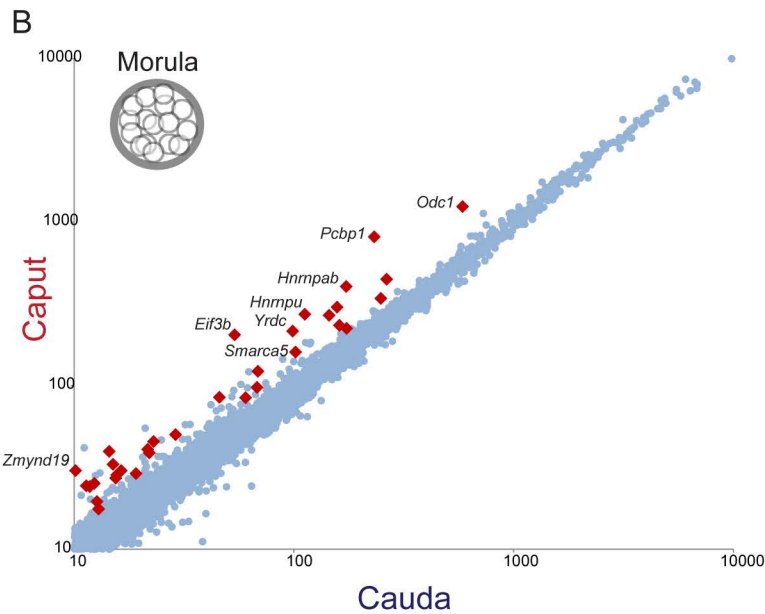
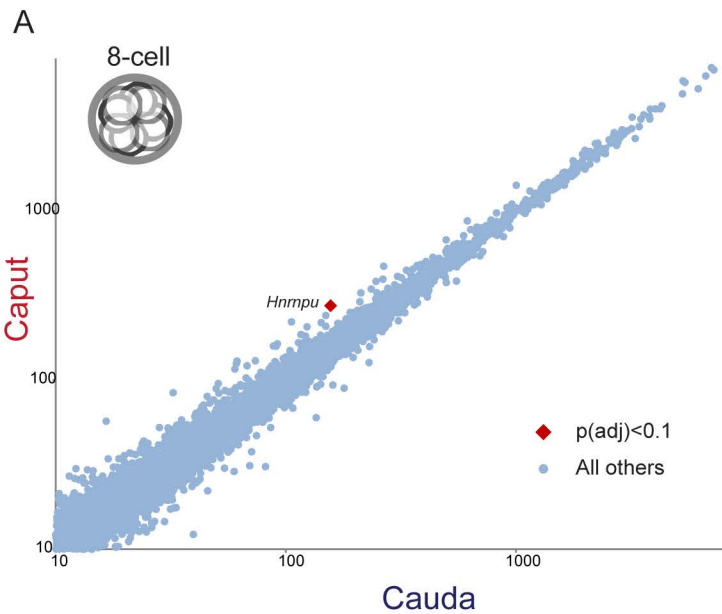
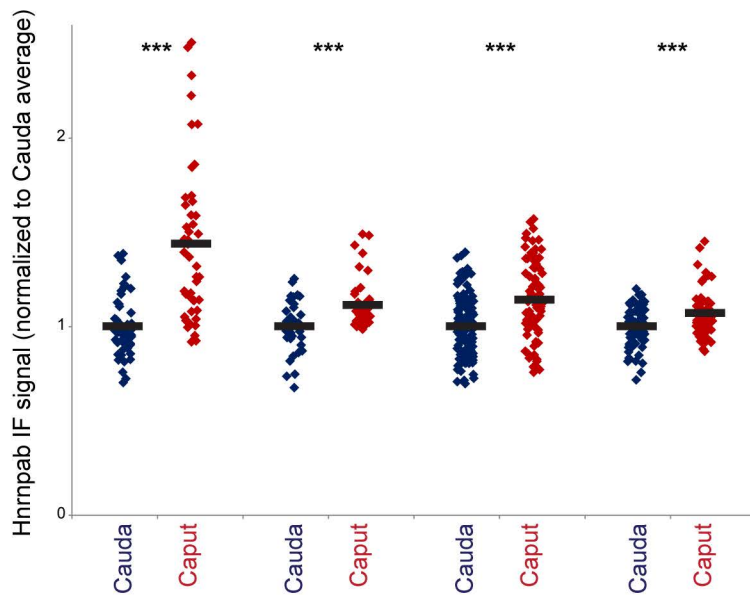




Figure S4

A



B

### Blastocyst stage gene expression

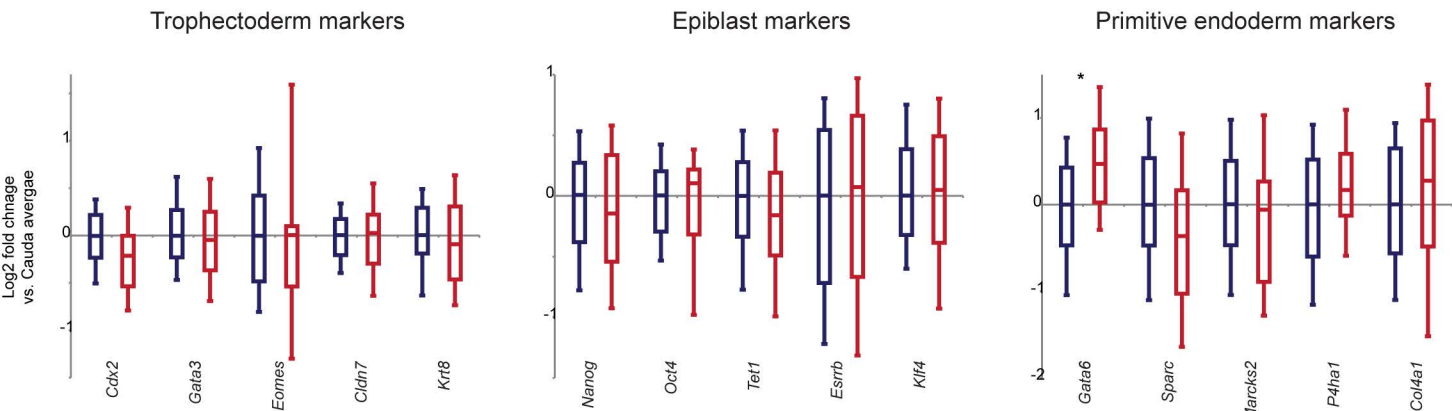


Figure S5

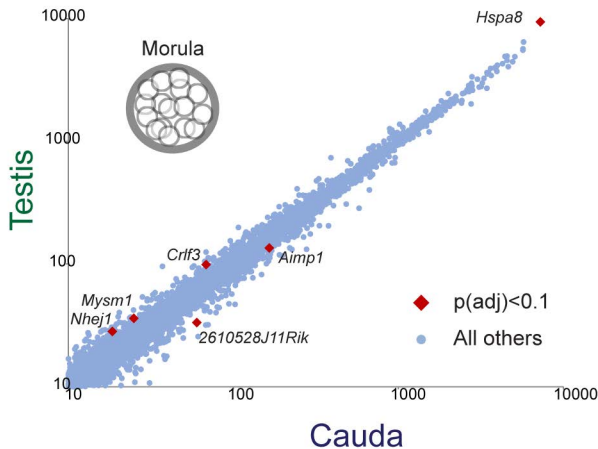
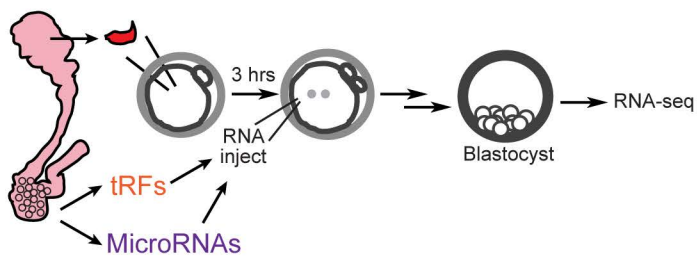


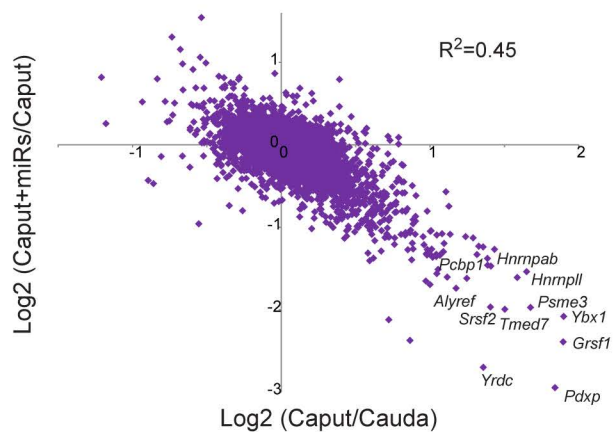


Figure S6

A



C



B

